

# A robust empirical relationship between speed and turbulence energy in the near-Earth solar wind

Rohit Chhiber<sup>1,2\*</sup>, Yanwen Wang<sup>3</sup>, Jiaming Wang<sup>1</sup>, and Sohom Roy<sup>4</sup>

<sup>1</sup>Department of Physics and Astronomy, University of Delaware, Newark, DE 19716, USA

<sup>2</sup>Heliophysics Science Division, NASA Goddard Space Flight Center, Greenbelt, MD 20771, USA

<sup>3</sup>Department of Physics, University of Maryland, College Park, MD 20742, USA

<sup>4</sup>Space Research Institute, Austrian Academy of Sciences, Schmiedlstraße 6, 8042, Graz, Austria

December 2, 2025

## Abstract

The connection between turbulence and solar-wind acceleration, long known in space physics, is further developed in this Letter by establishing a robust empirical law that relates the bulk-flow speed to the magnetohydrodynamic-scale fluctuation energy in the plasma. The model is based on analysis of twenty-five years of near-Earth observations by NASA’s Advanced Composition Explorer. It provides a simple way to estimate turbulence energy from low-resolution speed data – a practical approach that may be of utility when high-resolution measurements or advanced turbulence models are unavailable. Potential heliospheric applications include space-weather forecasting operations, remote imaging datasets, and energetic-particle transport models that require turbulence amplitudes to specify diffusion parameters.

## 1 Introduction

The solar wind is the continual dynamical outflow of plasma from the Sun into interplanetary space. It plays a fundamental role in physical processes occurring throughout the Solar System and is the main driver of the terrestrial impacts of space weather (Pulkkinen, 2007). The solar wind is also the only astrophysical system that can be accessed *in situ*, and as such, it serves as a unique and gigantic plasma laboratory in which scientists can investigate a variety of phenomena of relevance to astrophysics and plasma physics (e.g., Bruno and Carbone, 2013; Gurnett and Bhattacharjee, 2017).

The basic physical concepts of the solar wind have been known since its theoretical prediction by Parker (1958) and subsequent *in-situ* observation in the 1960s (for a historical review, see, e.g., Obridko and Vaisberg, 2017). Later studies have acknowledged the rich complexity of its structure and dynamics (e.g., Verscharen et al., 2019). Of particular note are questions relating to the heating and acceleration of the corona and the solar wind (Leer et al., 1982; Klimchuk, 2006, e.g.), and the transport of hazardous solar energetic particles (SEPs) and cosmic rays (CRs) through the heliosphere (e.g., Engelbrecht et al., 2022).

In recent decades, the study of waves and turbulence in the heliosphere has emerged as a major focus within the broader effort to address the above questions (Matthaeus and Velli, 2011). The turbulent

---

\*rohit.chhiber@nasa.gov, rohitc@udel.edu

cascade (e.g., Pope, 2000) provides an effective mechanism to account for non-adiabatic heating in weakly-collisional space plasmas (Kiyani et al., 2015; Matthaeus et al., 2020), and it is generally acknowledged that fast wind from coronal holes requires sustained acceleration over an extended region which can be provided by propagating Alfvén-wave-like fluctuations (e.g., De Pontieu et al., 2007; Cranmer, 2009; Rivera et al., 2024; Usmanov et al., 2025). Interplanetary turbulence can also account for the observed diffusive scattering of SEPs to distant heliolongitudes (e.g., Laitinen et al., 2016; Chhiber et al., 2021a) and directly induce geomagnetic activity (e.g., Borovsky and Funsten, 2003; D’Amicis et al., 2007), both effects of immediate interest to space weather forecasting operations (Bothmer and Daglis, 2007).

While the importance of turbulence in heliospheric phenomena has been recognized, incorporating turbulence within computational models of the solar wind and SEP transport has been challenging. Resolving the full range of spatio-temporal scales involved in magnetohydrodynamic (MHD) turbulence is computationally intractable for global three-dimensional simulations of the heliosphere (Miesch et al., 2015; Gombosi et al., 2018). In response, some global simulations have adopted a type of “subgrid” modeling approach that couples the resolved bulk flow with approximate statistical models of unresolved turbulence (e.g., Matthaeus et al., 1999; Usmanov et al., 2000; van der Holst et al., 2014; Shiota et al., 2017). By accounting for the low-frequency “energy containing” scales of turbulence (e.g., Zhou et al., 2004), these physics-based models reproduce a variety of observations, including non-adiabatic heating and fast wind speeds (e.g., Chhiber et al., 2021b; Usmanov et al., 2025). However, they are mathematically complex and computationally demanding; importantly, the latter aspect makes them unsuitable for real-time space weather forecasting and for community tools that provide “runs on request” (e.g., NASA’s CCMC<sup>1</sup>), which require relatively brief run time. The latter class of models typically employs empirical approaches like the Wang-Sheeley-Argé (WSA; Wang and Sheeley, 1990; Argé and Pizzo, 2000) relationship between magnetic flux-tube expansion and wind speed to produce fast solar wind streams, machine learning methods (e.g., Upendran et al., 2020), and/or polytropic equations or ad-hoc heating functions to obtain realistic temperatures (e.g., Pizzo et al., 2011; Sokolov et al., 2013; MacNeice et al., 2018; Samara et al., 2024). SEP forecasting models often use heuristic, constant turbulence levels (e.g., Hu et al., 2022; Whitman et al., 2023).

In this Letter we suggest an empirical approach that can be used to obtain reasonably accurate estimates of MHD turbulence levels simply from low-resolution (lo-res) speed data. It is based on an empirical law, derived from analysis of 25 years of near-Earth observations by NASA’s Advanced Composition Explorer (*ACE*) mission, that relates the bulk speed of the solar wind to its average turbulence energy. The approach can be useful in the aforementioned modeling frameworks that lack turbulence and also in extracting turbulence information from lo-res observations. Potential observational applications include sparse *in-situ* datasets from the outer heliosphere (e.g., *Voyager* and *New Horizons*; Elliott et al., 2016; Wrench and Parashar, 2025) and flow-speed maps derived from remote-sensing images (e.g., DeForest et al., 2025; Attie et al., 2025).

We bear in mind that a positive correlation between wind speed and turbulence levels has been noted in previous work (e.g., Forsyth et al., 1996; Horbury and Balogh, 2001; Erdős and Balogh, 2005; Shi et al., 2023; Usmanov et al., 2025), and it is believed to be related to magnetic topology at the solar source (Wang and Sheeley, 1991; Cranmer and Winebarger, 2019). However, to the best of our knowledge, the present study is the first time an empirical model based on this relationship has been derived and evaluated. We delve deeper into its physical origins in a companion paper (Chhiber et al. 2026, in prep.).

---

<sup>1</sup>Community Coordinated Modeling Center; <https://ccmc.gsfc.nasa.gov/>.

## 2 Data

We employ *in-situ* observations from *ACE*, situated at  $L_1$  and spanning the period from 1998-02-05 00:00:00 to 2023-12-31 23:59:00 (UTC). The magnetic field was obtained from the MAG instrument (Smith et al., 1998) and plasma data (ion number density and velocity) from the SWEPAM instrument (McComas et al., 1998). The downloaded magnetic data with 1-s resolution were downsampled to a 1-min cadence, while density and velocity data at 64-s were upsampled using linear interpolation to match the magnetic field’s cadence. These data span  $\sim 2.5$  solar activity cycles (Usoskin, 2023), including three maxima and two minima (see Fig. 3). Plasma measurements are sometimes unavailable; possible reasons for this include contamination by large CME/SEP events (Skoug et al., 2004), instrumental aging after 2010 (Skoug et al., 2014), or spacecraft attitude adjustment and calibration periods. The instrumental aging that affects proton density measurements was addressed in 2012 with adjustments to the spacecraft by the *ACE* team (see Skoug et al., 2014).

In our analysis missing data points are represented as ‘NaN’, and the full dataset is partitioned into consecutive non-overlapping 12-hour intervals that begin at 00:00 each day, closed at the start time and open at the end time. The NaNs mainly affect density data, which, for our analysis, are only required to compute the mean density within an interval (see Sec. 3). We exclude intervals in which the fraction of NaNs in density is above 90%. In the remaining intervals the fraction of NaNs in the velocity and magnetic field data is below 10%. The 12-hour interval duration is chosen to include several turbulent correlation times ( $\sim 1$  hour at 1 au; Bruno and Carbone, 2013), which is a standard approach when computing turbulence statistics (e.g., Matthaeus and Goldstein, 1982).<sup>2</sup>

We identify intervals containing interplanetary coronal mass ejections (ICMEs; Webb and Howard, 2012) by referencing a catalog compiled by Richardson and Cane (2010), which has been updated as recently as 2025 (Richardson and Cane, 2024); 1,270 such intervals are identified. The remainder of the intervals (10,661 in number) are considered to be representative of the ambient solar wind in near-Earth space, which is our focus here. The resulting *ACE* dataset has been employed in a number of recent studies by our group (Roy et al., 2021, 2022; Wang et al., 2024, 2025).

## 3 Results

To examine the correlation between bulk solar wind speed and turbulence energy we compute the mean speed for each 12-hour interval:  $V \equiv |\mathbf{V}| \equiv |\langle \tilde{\mathbf{V}} \rangle|$ , where the  $\langle \cdot \rangle$  operator indicates an arithmetic mean computed over an interval and  $\tilde{\cdot}$  represents a quantity at 1-min cadence (in this case the ion velocity  $\tilde{\mathbf{V}}$ ). The magnetic field  $\tilde{\mathbf{B}}$  is converted to Alfvén units:  $\tilde{\mathbf{B}}_A = \tilde{\mathbf{B}}/\sqrt{4\pi\rho}$  where  $\rho = m_p n \equiv m_p \langle \tilde{n} \rangle$  is the mean proton mass density of the interval, computed from the proton mass  $m_p$  and the ion number density  $\tilde{n}$ . Hereafter, it is understood that the magnetic field is in Alfvén units and we drop the subscript ‘A’. Magnetic and velocity fluctuations are computed using a standard approach (e.g., Pope, 2000; Chhiber et al., 2021b):  $\tilde{\mathbf{v}} = \tilde{\mathbf{V}} - \mathbf{V}$  and  $\tilde{\mathbf{b}} = \tilde{\mathbf{B}} - \mathbf{B}$ , where  $\mathbf{B} \equiv \langle \tilde{\mathbf{B}} \rangle$  is the mean magnetic field in an interval. The average energies per-unit-mass in magnetic and velocity fluctuations are then  $\langle \tilde{v}^2 \rangle/2$  and  $\langle \tilde{b}^2 \rangle/2$ , respectively, and (twice) the total turbulent energy is  $Z^2 = v^2 + b^2$ , where we have defined  $v^2 \equiv \langle \tilde{v}^2 \rangle$  and  $b^2 \equiv \langle \tilde{b}^2 \rangle$  as the mean-squared fluctuations.<sup>3</sup> Note that our averaging procedure obtains information about the energy-containing scales of turbulence, at which the largest turbulent structures (or “eddies”) inject energy into the inertial-range cascade (e.g., Pope, 2000; Kiyani et al., 2015; Bandyopadhyay et al., 2020; Wu et al., 2022).

<sup>2</sup>We have repeated our analysis (Sec. 3) for 6 and 24 hour intervals, and by excluding intervals in which the fraction of NaNs in density data is above 70%. The results are not significantly changed in any of these cases.

<sup>3</sup>We neglect density fluctuations since inner-heliospheric turbulence is believed to be nearly incompressible (Belcher and Davis, 1971; Matthaeus et al., 1990; Zank et al., 2017).

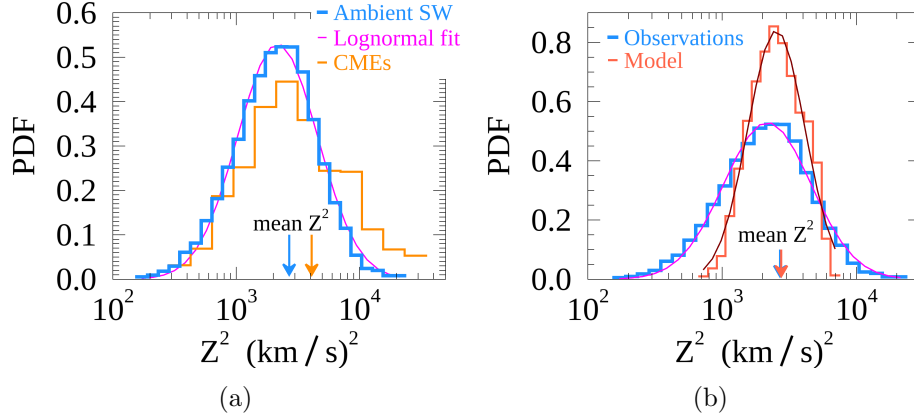


Figure 1: Probability density functions (PDFs) of log of turbulence energy ( $\log Z^2$ ), with horizontal axes showing corresponding  $Z^2$  values on a logarithmic scale. (a): Thick blue histogram is for ambient solar wind (sw) intervals and thin orange histogram is for intervals that include ICMEs. Best-fit Gaussian to  $\log Z^2$  (i.e., a log-normal fit to  $Z^2$ ) for the ambient sw is shown as a magenta curve. Sample means are marked with arrows of corresponding color; with  $1\sigma$  spread, these are  $2.7 \pm 2.1 \times 10^3$  (km/s) $^2$  and  $4.1 \pm 4.0 \times 10^3$  (km/s) $^2$ , respectively. (b) The observed PDF for ambient sw is compared with the PDF obtained from the modeled  $Z^2$  (thin tomato-colored histogram) and its best-fit log-normal (maroon curve). The model shown here is the quadratic fit (see Table 1). Sample means for the two cases are marked with arrows as in (a); these almost overlap. The model  $1\sigma$  is  $1.2 \times 10^3$  (km/s) $^2$ . Gaussian fits are performed using the IDL function `gaussfit.pro`.

Fig. 1(a) shows probability density functions (PDFs) of  $\log Z^2$  for the ambient and CME intervals. Although our focus remains on the former, we note that the CME distribution is shifted to larger  $Z^2$  and has a mean that is  $\sim 40\%$  greater than that for the ambient intervals, which is qualitatively consistent with a recent study by Good et al. (2023). Both PDFs have large variance and appear to follow log-normal distributions (i.e.,  $\log Z^2$  is normally distributed; Limpert et al., 2001), as is often the case with turbulence properties observed in the heliosphere (e.g., Burlaga and Lazarus, 2000; Padhye et al., 2001; Ruiz et al., 2014; Pradata et al., 2025; Chhiber et al., 2025). A best-fit log-normal to the blue PDF shows very good agreement. Fig. 1(b) is discussed below.

Fig. 2 shows colormaps of two-dimensional (2D) joint histograms of  $V$  paired with three turbulent quantities. A clear positive correlation is apparent between mean speed and the two turbulence energies,  $Z^2$  and  $b^2$ . The Pearson correlation coefficients (PCCs) between  $V$  and  $\log Z^2$  and  $\log b^2$  are 0.59 and 0.56, respectively. Empirical fits to three different functions are shown, with fit parameters specified in Table 1. The quadratic and linear fits hardly differ in the core of the distribution, and the former has the lowest mean-squared error of three (unsurprisingly, with its three free parameters). The ratio of velocity and magnetic fluctuation energies, called the Alfvén ratio ( $r_A = v^2/b^2$ ), indicates relatively smaller variation compared with the turbulence energies; its mean changes from  $\sim 0.4$  in slow wind ( $V \lesssim 500$  km/s) to  $\sim 0.6$  at faster wind speeds, consistent with previous studies (Bruno and Carbone, 2013).

In addition to  $Z^2$ , we have also shown the fit of  $b^2$  to  $V$  and the joint distribution of  $r_A$  and  $V$ , since energetic-particle diffusion coefficients are usually expressed in terms of  $b^2$  (e.g., Engelbrecht et al., 2022). In our suggested approach, the latter quantity can either be obtained from the  $Z^2$  fit to  $V$  by specifying  $r_A$  (as is commonly done in studies that apply solar wind models to CR/SEP transport; e.g., Guo and Florinski, 2016; Chhiber et al., 2017), or directly from the  $b^2$  fit to  $V$ . Note that this approach will yield the magnetic fluctuation energy in Alfvén units, which can then be converted to magnetic-field units using (readily available) density data.

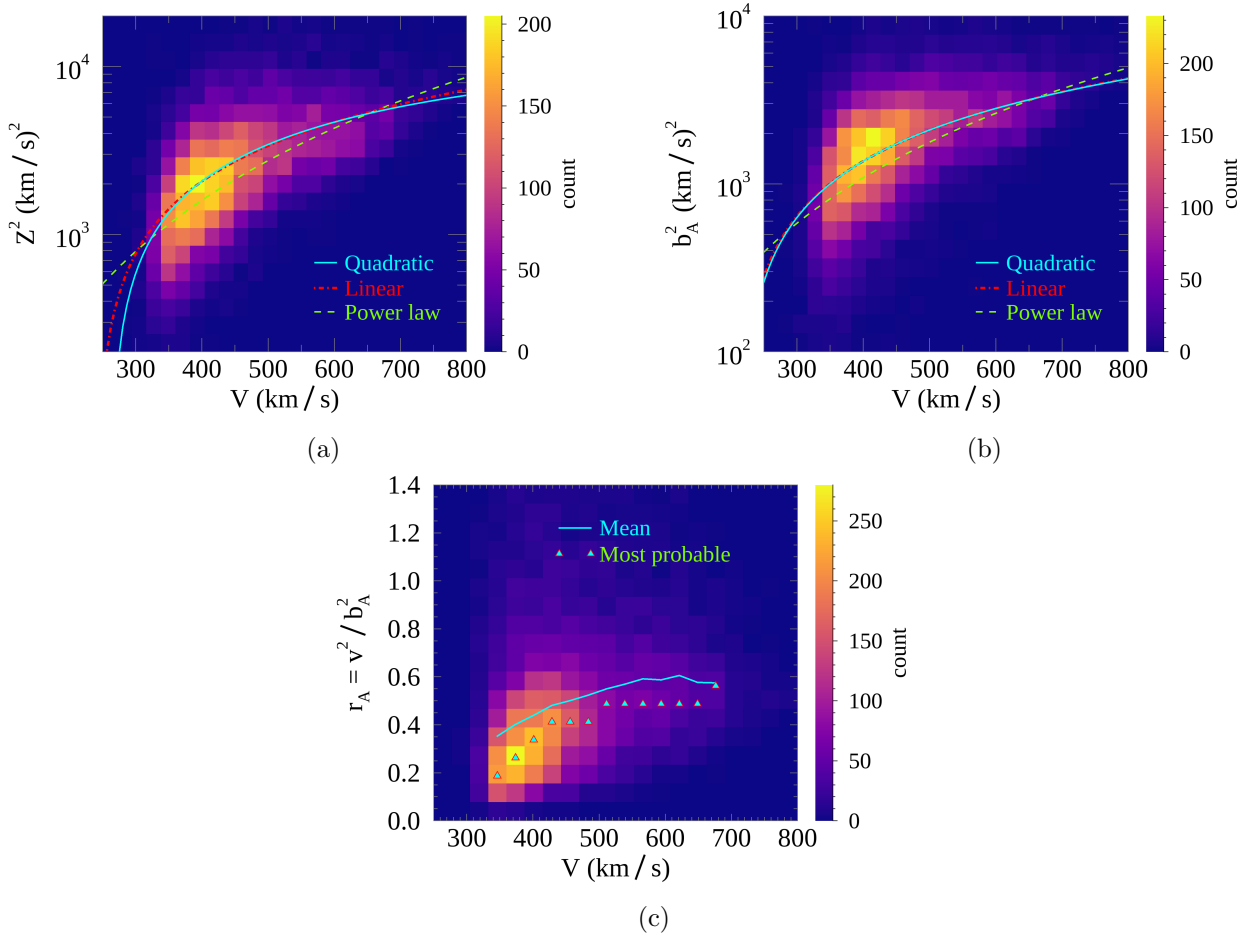


Figure 2: Joint histograms of mean speed  $V$  and (a) total turbulence energy  $Z^2$ , (b) magnetic turbulence energy  $b_A^2 \equiv b^2$ , and (c) Alfvén ratio  $r_A$ . Colorbars show interval abundance. Panels (a) and (b) show three empirical fits each of  $Z^2$  and  $b_A^2$  to  $V$ , respectively. Fit parameters are stated in Table 1. Panel (c) shows the mean and most probable values of  $r_A$  in bins of  $V$ .

$y$	Quadratic: $y = A_0 + A_1V + A_2V^2$			Linear: $y = B_0 + B_1V$		Power law: $y = C_0V^{C_1}$	
	$A_0$	$A_1$	$A_2$	$B_1$	$B_2$	$C_1$	$C_2$
$Z^2$	$-4633 \pm 521$	$19.3 \pm 2.1$	$-0.006 \pm 0.002$	$-3126 \pm 111$	$13.0 \pm 0.2$	$0.0007 \pm 0.1872$	$2.43 \pm 0.03$
$b^2$	$-1625 \pm 269$	$7.6 \pm 1.1$	$-0.0004 \pm 0.0011$	$-1527 \pm 58$	$7.2 \pm 0.1$	$0.002 \pm 0.185$	$2.17 \pm 0.03$

Table 1: Empirical fit parameters with  $1\sigma$  uncertainty estimates for  $y = Z^2$  and  $y = b^2$ , as functions of  $V$ . Fitting was based on the full 25-year dataset (cf. Fig. 3). Units of coefficients are consistent with  $y$  in (km/s) $^2$  and  $V$  in km/s. Quadratic fitting was performed using the IDL function `poly_fit.pro`, and linear and power-law fits were obtained using the IDL function `linfit.pro`. A cubic fit was also performed but was indistinguishable from the quadratic one.

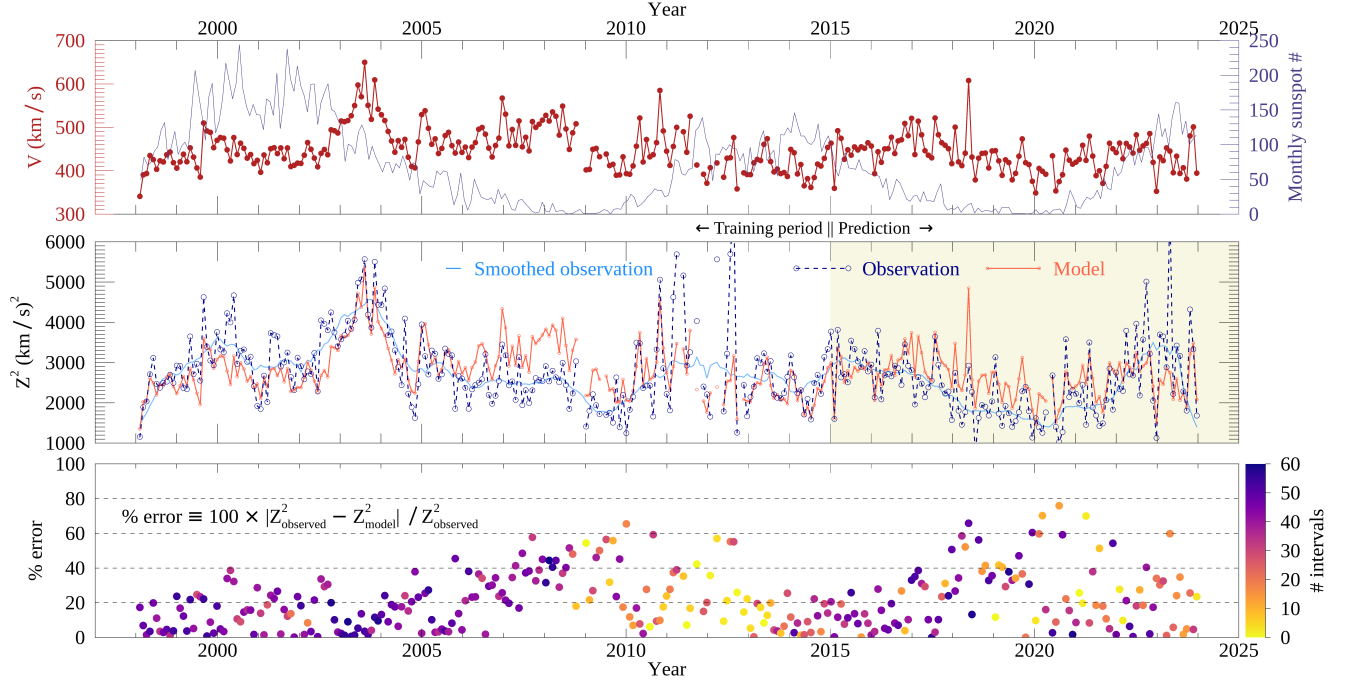


Figure 3: Evaluation of model performance over a 25-year period. *Top panel:* For context, mean solar-wind speed is shown at 30-day cadence (see text) as brown connected circles that map to the left vertical axis. Monthly averages of solar sunspot number are shown as dark blue curve that maps to the right vertical axis. *Middle panel:* Dashed dark-blue curve with circles shows observed  $Z^2$  at 30-day cadence; light-blue solid curve shows a 360-day running average. Red curve shows the modeled  $Z^2$  at 30-day cadence. Here, model values are obtained from a quadratic fit -  $Z^2 = A_0 + A_1V + A_2V^2$  - based on observations preceding 2015, i.e., from the annotated “Training period”;  $A_0 = -3533$ ,  $A_1 = 15$ ,  $A_2 = -0.002$  (cf. Table 1). Model values after the training period constitute a type of prediction, shown on a beige-shaded background. PCC between the 30-day cadence observations and model values is 0.61. *Bottom panel:* Circles show percentage error between observed and modeled values of  $Z^2$ , at 30-day cadence. Color of circles maps to colorbar on the right, indicating number of 12-hour intervals within each 30-day period represented by a circle.

For a statistical comparison of the model-generated values with the observed  $Z^2$ , we plot the PDFs of the two in Fig. 1(b); model values are computed from the mean speed of each interval using the quadratic fit (Table 1). Consistent with the observations, the model produces log-normally distributed  $Z^2$ , with a sample mean that is nearly identical to that of the observations. Modeled values have a notably smaller spread, with a standard deviation that is half of the observed value.

The model’s performance is further evaluated in Fig. 3. The top panel provides context, showing the mean solar-wind speed for the 25-year period; here the 12-hour cadence time-series of mean speed computed from ambient solar wind intervals is smoothed using a moving boxcar average spanning 30-days, and the result is plotted at a 30-day cadence. Also shown are monthly averages of the solar sunspot number obtained from Clette and Lefèvre (2015).

The middle panel shows a comparison of the observed  $Z^2$  (plotted at 30-day cadence, as above) with the quadratic model. To demonstrate the robustness of the model and to showcase its applicability to time periods beyond those in which the fitting was performed, for this figure we have computed a

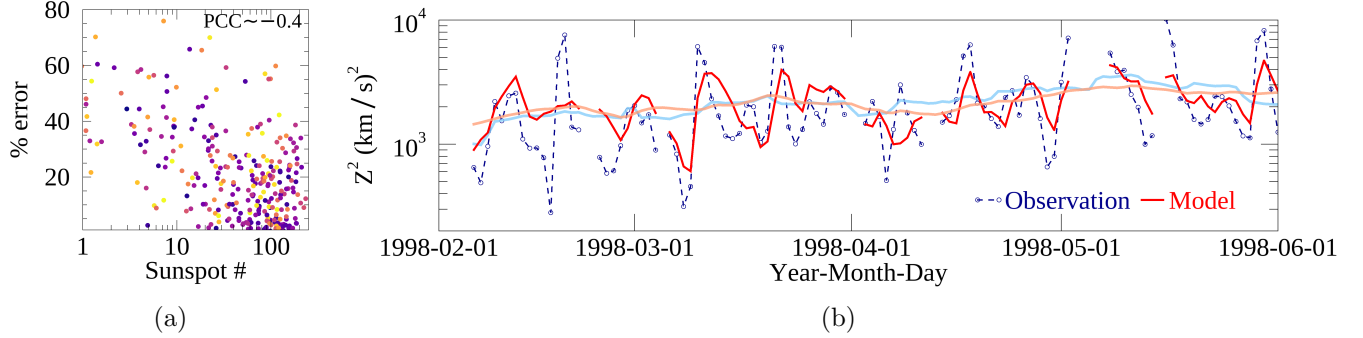


Figure 4: (a) Scatterplot of percent error between modeled and observed  $Z^2$ , and monthly sunspot number (both from Fig. 3). The PCC is  $-0.37$ . Colors of circles map to colorbar in Fig. 3. (b) A “zoomed in” comparison of observed and modeled  $Z^2$ , spanning a period of around 4 months. Dashed dark-blue curve with circles shows observations at a 1-day cadence, with the corresponding (quadratic) model curve in red. Pale blue and red curves show the respective 10-day running averages. The PCC between the daily observations and model values is 0.61.

best-fit quadratic based on observations preceding 2015, defining a “training period”.<sup>4</sup> Then the model values from 2015 onward constitute a type of prediction. Overall, the model appears to give a good-to-reasonable agreement with observations in both the training and prediction periods. There are instances of remarkably detailed quantitative agreement for a range of observed  $Z^2$  (and speed), while a few instances indicate discrepancy by a factor of  $\sim 2$ . The PCC between the 30-day cadenced observations and the model values is 0.61. The 360-day smoothed observation (light blue curve) indicates that the model follows the observed long-term trends. We note that some observational periods are highly “noisy”, with large spikes in the dashed blue curve. This is likely related to a paucity of observations in those periods, as discussed below. We also note a moderate correlation between sunspot number and observed turbulence energy, with a PCC of  $\sim 0.4$ .

The bottom panel of Fig. 3 shows the percentage error between the observed and modeled  $Z^2$ ; this is generally below 20% for around half of the 25-year period, but there are periods when it becomes more variable, reaching 60% on occasion. There is a moderate anti-correlation between sunspot number and the error (PCC  $-0.37$ ), seen also in the scatter plot in Fig. 4(a). This suggests that the model may perform better during solar maximum when *ACE* is more likely to sample coronal-hole wind (e.g., McComas et al., 2003); further study will be required on this point. We note that the model’s better performance during solar maximum makes it suitable for application to SEP forecasting, since these events are more numerous during high solar activity.

The color of the circles in the bottom panel of Fig. 3 indicates the number of 12-hour intervals that were available within each 30-day period represented by a circle. It is evident that the spiky values of observed  $Z^2$  in the middle panel tend to occur when there is a paucity of intervals (indicated by light-colored circles). The factors that produce the observed variations in the number of intervals were discussed in Sec. 2.

Finally, Fig. 4(b) shows a “zoomed in” comparison of observed and modeled  $Z^2$ , both evaluated at a daily cadence in this instance, using an approach analogous to the one used to produce the 30-day cadence values above. Even at these much shorter timescales (compared to those in Fig. 3) there are periods of remarkably good agreement, and the 10-day running averages overlap well. The PCC between observations and modeled values (at daily cadence) is 0.61.

<sup>4</sup>The parameters of this fit (see Fig. 3 caption) are not significantly different from those obtained from the full 25-year dataset (Table 1).

## 4 Conclusions

In this Letter we have examined the relationship between bulk flow speed and turbulence energy in the near-Earth solar wind, by analyzing 25 years of *ACE* observations. The key result is an empirical law that produces reasonably accurate predictions of the average turbulence energy, simply from coarse-grained speed data. We suggest that the current approach (likely the first of its type, although similar in spirit to the widely-used WSA model) has the potential to enhance the capabilities of operational space-weather models and other datasets that are typically not considered suitable for turbulence studies. For example, SEP forecasting models can leverage their speed data to obtain self-consistent and data-constrained estimates of turbulence energy, which is a crucial parameter for modeling SEP diffusion (e.g., Engelbrecht et al., 2022; Hu et al., 2022; Whitman et al., 2023). Our empirical model may also be useful in global MHD simulations of the heliosphere that lack turbulence modeling (e.g., Provornikova et al., 2024; Samara et al., 2024). Following further validation of the empirical law(s) at greater/smaller helioradii (e.g., Shi et al., 2023) and outside the ecliptic plane (e.g., McComas et al., 2003), they can be applied to global flow maps from remote-imaging instruments like *PUNCH* (DeForest et al., 2025; Attie et al., 2025) to extract turbulence levels spanning the meridional plane (e.g., Usmanov et al., 2025). We note that the observed positive correlation between speed and turbulence amplitude may be relevant to geomagnetic activity, which is known to be driven by high-speed streams (D’Amicis et al., 2007; Baker et al., 2018).

In addition to validation of the empirical model(s) in heliospheric regions beyond near-Earth space, future work can also investigate its apparent superior performance during solar maximum. It is likely that the observed speed-turbulence correlation is related to the well-known correlation between speed and proton temperature (e.g., Matthaeus et al., 2006; Elliott et al., 2012; Shi et al., 2023); further study of these correlations can help improve our understanding of the role of turbulence in solar wind acceleration and heating.

---

## Data Sources

*ACE* magnetic field data were downloaded from <https://spdf.gsfc.nasa.gov/pub/data/ace/mag/level2cdaweb/mfih3/> and plasma data were downloaded from [https://spdf.gsfc.nasa.gov/pub/data/ace/swepam/level2\\_hdf/ions\\_64sec](https://spdf.gsfc.nasa.gov/pub/data/ace/swepam/level2_hdf/ions_64sec). The ICME list is available at <https://doi.org/10.7910/DVN/C2MHTH>. Sunspot-number data was obtained from the World Data Center SILSO, Royal Observatory of Belgium, Brussels, <https://doi.org/10.24414/qnza-ac80>.

## Acknowledgements

This research was supported by NASA under the Living With a Star (LWS) Science program grant 80NSSC22K1020, and utilized resources provided by the National Energy Research Scientific Computing Center (NERSC).

## References

- C. N. Arge and V. J. Pizzo. Improvement in the prediction of solar wind conditions using near-real time solar magnetic field updates. *J. Geophys. Res.*, 105(A5):10465–10480, May 2000. doi: 10.1029/1999JA000262.
- Raphael Attie, Valmir Moraes Filho, Barbara Thompson, Vadim Uritsky, Nicholeen Viall, Craig DeForest, Heather Elliott, Maher Dayeh, and Chadi Salem. Tracking the Multiscale Solar Wind Evolution with



- PUNCH Flow Maps. In *246th Meeting of the American Astronomical Society*, volume 246 of *American Astronomical Society Meeting Abstracts*, page 126.05, June 2025.
- D. N. Baker, P. J. Erickson, J. F. Fennell, J. C. Foster, A. N. Jaynes, and P. T. Verronen. Space Weather Effects in the Earth’s Radiation Belts. *Space Sci. Rev.*, 214(1):17, February 2018. doi: 10.1007/s11214-017-0452-7.
- Riddhi Bandyopadhyay, M. L. Goldstein, B. A. Maruca, W. H. Matthaeus, T. N. Parashar, D. Ruffolo, R. Chhiber, A. Usmanov, A. Chasapis, R. Qudsi, Stuart D. Bale, J. W. Bonnell, Thierry Dudok de Wit, Keith Goetz, Peter R. Harvey, Robert J. MacDowall, David M. Malaspina, Marc Pulupa, J. C. Kasper, K. E. Korreck, A. W. Case, M. Stevens, P. Whittlesey, D. Larson, R. Livi, K. G. Klein, M. Velli, and N. Raouafi. Enhanced Energy Transfer Rate in Solar Wind Turbulence Observed near the Sun from Parker Solar Probe. *ApJS*, 246(2):48, February 2020. doi: 10.3847/1538-4365/ab5dae.
- J. W. Belcher and L. Davis, Jr. Large-amplitude Alfvén waves in the interplanetary medium, 2. *J. Geophys. Res.*, 76:3534, 1971. doi: 10.1029/JA076i016p03534.
- Joseph E. Borovsky and Herbert O. Funsten. Role of solar wind turbulence in the coupling of the solar wind to the Earth’s magnetosphere. *Journal of Geophysical Research (Space Physics)*, 108(A6):1246, June 2003. doi: 10.1029/2002JA009601.
- Volker Bothmer and Ioannis A Daglis. *Space weather: physics and effects*. Springer Berlin, Heidelberg, 2007.
- R. Bruno and V. Carbone. The Solar Wind as a Turbulence Laboratory. *Living Reviews in Solar Physics*, 10:2, December 2013. doi: 10.12942/lrsp-2013-2.
- L. F. Burlaga and A. J. Lazarus. Lognormal distributions and spectra of solar wind plasma fluctuations: Wind 1995-1998. *J. Geophys. Res.*, 105(A2):2357–2364, February 2000. doi: 10.1029/1999JA900442.
- R. Chhiber, P. Subedi, A. V. Usmanov, W. H. Matthaeus, D. Ruffolo, M. L. Goldstein, and T. N. Parashar. Cosmic-Ray Diffusion Coefficients throughout the Inner Heliosphere from a Global Solar Wind Simulation. *ApJS*, 230:21, June 2017. doi: 10.3847/1538-4365/aa74d2.
- Rohit Chhiber, David Ruffolo, William H. Matthaeus, Arcadi V. Usmanov, Paisan Tooprakai, Piyanate Chuychai, and Melvyn L. Goldstein. Random Walk and Trapping of Interplanetary Magnetic Field Lines: Global Simulation, Magnetic Connectivity, and Implications for Solar Energetic Particles. *ApJ*, 908(2):174, February 2021a. doi: 10.3847/1538-4357/abd7f0.
- Rohit Chhiber, Arcadi V. Usmanov, William H. Matthaeus, and Melvyn L. Goldstein. Large-scale Structure and Turbulence Transport in the Inner Solar Wind: Comparison of Parker Solar Probe’s First Five Orbits with a Global 3D Reynolds-averaged MHD Model. *ApJ*, 923(1):89, December 2021b. doi: 10.3847/1538-4357/ac1ac7.
- Rohit Chhiber, Raphael Attie, William H. Matthaeus, Sohom Roy, and Barbara J. Thompson. von Kármán-Howarth Similarity of Spatial Correlations and the Distribution of Correlation Lengths in Solar Photospheric Turbulence. *MNRAS*, October 2025. doi: 10.1093/mnras/staf1863.
- F. Clette and L. Lefèvre. Silso sunspot number v2.0. <https://doi.org/10.24414/qnza-ac80>, 07 2015. Published by WDC SILSO - Royal Observatory of Belgium (ROB).
- Steven R. Cranmer. Coronal Holes. *Living Reviews in Solar Physics*, 6(1):3, December 2009. doi: 10.12942/lrsp-2009-3.

- Steven R. Cranmer and Amy R. Winebarger. The Properties of the Solar Corona and Its Connection to the Solar Wind. *ARA&A*, 57:157–187, August 2019. doi: 10.1146/annurev-astro-091918-104416.
- R. D’Amicis, R. Bruno, and B. Bavassano. Is geomagnetic activity driven by solar wind turbulence? *Geophys. Res. Lett.*, 34(5):L05108, March 2007. doi: 10.1029/2006GL028896.
- B. De Pontieu, S. W. McIntosh, M. Carlsson, V. H. Hansteen, T. D. Tarbell, C. J. Schrijver, A. M. Title, R. A. Shine, S. Tsuneta, Y. Katsukawa, K. Ichimoto, Y. Suematsu, T. Shimizu, and S. Nagata. Chromospheric Alfvénic Waves Strong Enough to Power the Solar Wind. *Science*, 318(5856):1574, December 2007. doi: 10.1126/science.1151747.
- Craig DeForest, Sarah Gibson, Ronnie Killough, Nick Waltham, Matt Beasley, Robin Colaninno, Glenn Laurent, Daniel Seaton, Marcus Hughes, Madhulika Guhathakurta, Nicholeen Viall, Raphael Attie, Dipankar Banerjee, Luke Barnar, Doug Biesecker, Mario Bisi, Volker Bothmer, Antonina Brody, Joan Burkepille, Iver Cairns, Jennifer Campbell, david Cheney, Traci Case, Amir Caspi, Rohit Chhiber, Matthew Clapp, Steven Cranmer, Jackie Davies, Curt de Koning, Mihir Desai, Heather Elliott, Samaiyah Farid, Bea Gallardo-Lacourt, Chris Gilly, Caden Gobat, Mary Hanson, Richard Harrison, Donald Hassler, Chase Henley, Alan Henry, Russell Howard, Bernard Jackson, Samuel Jones, Don Kolinski, Derek Lamb, Florine Lehtinen, Chris Lowder, Anna Malanushenko, William Matthaeus, David McComas, Jacob McGee, Huw Morgan, Divya Oberoi, Dusan Odstrcil, Chris Parmenter, Ritesh Patel, Francesco Pecora, Steve Persyn, Victor Pizzo, Simon Plunkett, Elena Provornikova, Nour Eddine Raouafi, Jillian Redfern, Alexis Rouillard, Kelly Smith, Keith Smith, Zachary Talpas, James Tappin, Arnaud Thernisien, Barbara Thompson, Samuel Van Kooten, Kevin Walsh, David Webb, William Wells, Matthew West, Zachary Wiens, and Yan Yang. Polarimeter to Unify the Corona and Heliosphere (PUNCH). *arXiv e-prints*, art. arXiv:2509.15131, September 2025. doi: 10.48550/arXiv.2509.15131.
- H. A. Elliott, C. J. Henney, D. J. McComas, C. W. Smith, and B. J. Vasquez. Temporal and radial variation of the solar wind temperature-speed relationship. *Journal of Geophysical Research (Space Physics)*, 117(A9):A09102, September 2012. doi: 10.1029/2011JA017125.
- H. A. Elliott, D. J. McComas, P. Valek, G. Nicolaou, S. Weidner, and G. Livadiotis. The New Horizons Solar Wind Around Pluto (SWAP) Observations of the Solar Wind from 11-33 au. *ApJS*, 223(2):19, April 2016. doi: 10.3847/0067-0049/223/2/19.
- N. Eugene Engelbrecht, F. Effenberger, V. Florinski, M. S. Potgieter, D. Ruffolo, R. Chhiber, A. V. Usmanov, J. S. Rankin, and P. L. Els. Theory of Cosmic Ray Transport in the Heliosphere. *Space Sci. Rev.*, 218(4):33, June 2022. doi: 10.1007/s11214-022-00896-1.
- Géza Erdős and André Balogh. In situ observations of magnetic field fluctuations. *Advances in Space Research*, 35(4):625–635, January 2005. doi: 10.1016/j.asr.2005.02.048.
- R. J. Forsyth, T. S. Horbury, A. Balogh, and E. J. Smith. Hourly variances of fluctuations in the heliospheric magnetic field out of the ecliptic plane. *Geophys. Res. Lett.*, 23(5):595–598, March 1996. doi: 10.1029/96GL00416.
- T. I. Gombosi, B. van der Holst, W. B. Manchester, and I. V. Sokolov. Extended MHD modeling of the steady solar corona and the solar wind. *Living Reviews in Solar Physics*, 15:4, July 2018. doi: 10.1007/s41116-018-0014-4.
- S. W. Good, O. K. Rantala, A.-S. M. Jylhä, C. H. K. Chen, C. Möstl, and E. K. J. Kilpua. Turbulence Properties of Interplanetary Coronal Mass Ejections in the Inner Heliosphere: Dependence on Proton Beta and Flux Rope Structure. *ApJL*, 956(1):L30, October 2023. doi: 10.3847/2041-8213/acfd1c.

- X. Guo and V. Florinski. Galactic Cosmic-Ray Intensity Modulation by Corotating Interaction Region Stream Interfaces at 1 au. *ApJ*, 826:65, July 2016. doi: 10.3847/0004-637X/826/1/65.
- Donald A Gurnett and Amitava Bhattacharjee. *Introduction to plasma physics: With space, laboratory and astrophysical applications*. Cambridge University Press, Cambridge, 2017.
- T. S. Horbury and A. Balogh. Evolution of magnetic field fluctuations in high-speed solar wind streams: Ulysses and Helios observations. *J. Geophys. Res.*, 106(A8):15929–15940, August 2001. doi: 10.1029/2000JA000108.
- Junxiang Hu, Vladimir S. Airapetian, Gang Li, Gary Zank, and Meng Jin. Extreme energetic particle events by superflare-associated CMEs from solar-like stars. *Science Advances*, 8(12):eabi9743, March 2022. doi: 10.1126/sciadv.abi9743.
- K. H. Kiyani, K. T. Osman, and S. C. Chapman. Dissipation and heating in solar wind turbulence: from the macro to the micro and back again. *Philosophical Transactions of the Royal Society of London Series A*, 373(2041):20140155–20140155, April 2015. doi: 10.1098/rsta.2014.0155.
- J. A. Klimchuk. On Solving the Coronal Heating Problem. *Sol. Phys.*, 234:41–77, March 2006. doi: 10.1007/s11207-006-0055-z.
- T. Laitinen, A. Kopp, F. Effenberger, S. Dalla, and M. S. Marsh. Solar energetic particle access to distant longitudes through turbulent field-line meandering. *A&A*, 591:A18, June 2016. doi: 10.1051/0004-6361/201527801.
- E. Leer, T. E. Holzer, and T. Fla. Acceleration of the solar wind. *Space Sci. Rev.*, 33:161–200, March 1982. doi: 10.1007/BF00213253.
- Eckhard Limpert, Werner A. Stahel, and Markus Abbt. Log-normal distributions across the sciences: Keys and clues: On the charms of statistics, and how mechanical models resembling gambling machines offer a link to a handy way to characterize log-normal distributions, which can provide deeper insight into variability and probability—normal or log-normal: That is the question. *BioScience*, 51(5):341–352, 05 2001. ISSN 0006-3568. doi: 10.1641/0006-3568(2001)051[0341:LNDATS]2.0.CO;2. URL [https://doi.org/10.1641/0006-3568\(2001\)051\[0341:LNDATS\]2.0.CO;2](https://doi.org/10.1641/0006-3568(2001)051[0341:LNDATS]2.0.CO;2).
- P. MacNeice, L. K. Jian, S. K. Antiochos, C. N. Arge, C. D. Bussy-Virat, M. L. DeRosa, B. V. Jackson, J. A. Linker, Z. Mikic, M. J. Owens, A. J. Ridley, P. Riley, N. Savani, and I. Sokolov. Assessing the Quality of Models of the Ambient Solar Wind. *Space Weather*, 16(11):1644–1667, November 2018. doi: 10.1029/2018SW002040.
- W. H. Matthaeus and M. L. Goldstein. Measurement of the rugged invariants of magnetohydrodynamic turbulence in the solar wind. *J. Geophys. Res.*, 87:6011–6028, August 1982. doi: 10.1029/JA087iA08p06011.
- W. H. Matthaeus and M. Velli. Who Needs Turbulence?. A Review of Turbulence Effects in the Heliosphere and on the Fundamental Process of Reconnection. *Space Sci. Rev.*, 160:145–168, October 2011. doi: 10.1007/s11214-011-9793-9.
- W. H. Matthaeus, M. L. Goldstein, and D. A. Roberts. Evidence for the presence of quasi-two-dimensional nearly incompressible fluctuations in the solar wind. *J. Geophys. Res.*, 95:20673–20683, December 1990. doi: 10.1029/JA095iA12p20673.

- W. H. Matthaeus, G. P. Zank, S. Oughton, D. J. Mullan, and P. Dmitruk. Coronal Heating by Magnetohydrodynamic Turbulence Driven by Reflected Low-Frequency Waves. *ApJL*, 523:L93–L96, September 1999. doi: 10.1086/312259.
- W. H. Matthaeus, H. A. Elliott, and D. J. McComas. Correlation of speed and temperature in the solar wind. *Journal of Geophysical Research (Space Physics)*, 111(A10):A10103, October 2006. doi: 10.1029/2006JA011636.
- William H. Matthaeus, Yan Yang, Minping Wan, Tulasi N. Parashar, Riddhi Bandyopadhyay, Alexandros Chasapis, Oreste Pezzi, and Francesco Valentini. Pathways to Dissipation in Weakly Collisional Plasmas. *Astrophys. J.*, 891(1):101, March 2020. doi: 10.3847/1538-4357/ab6d6a.
- D. J. McComas, H. A. Elliott, N. A. Schwadron, J. T. Gosling, R. M. Skoug, and B. E. Goldstein. The three-dimensional solar wind around solar maximum. *Geophys. Res. Lett.*, 30:1517, May 2003. doi: 10.1029/2003GL017136.
- DJ McComas, SJ Bame, P Barker, WC Feldman, JL Phillips, P Riley, and JW Griffee. Solar wind electron proton alpha monitor (swepam) for the advanced composition explorer. *Space Science Reviews*, 86(1): 563–612, 1998.
- M. Miesch, W. Matthaeus, A. Brandenburg, A. Petrosyan, A. Pouquet, C. Cambon, F. Jenko, D. Uzdensky, J. Stone, S. Tobias, J. Toomre, and M. Velli. Large-Eddy Simulations of Magnetohydrodynamic Turbulence in Heliophysics and Astrophysics. *Space Sci. Rev.*, 194:97–137, November 2015. doi: 10.1007/s11214-015-0190-7.
- V. N. Obridko and O. L. Vaisberg. On the history of the solar wind discovery. *Solar System Research*, 51:165–169, March 2017. doi: 10.1134/S0038094617020058.
- N. S. Padhye, C. W. Smith, and W. H. Matthaeus. Distribution of magnetic field components in the solar wind plasma. *J. Geophys. Res.*, 106(A9):18635–18650, September 2001. doi: 10.1029/2000JA000293.
- E. N. Parker. Dynamics of the Interplanetary Gas and Magnetic Fields. *ApJ*, 128:664, November 1958. doi: 10.1086/146579.
- Vic Pizzo, George Millward, Annette Parsons, Douglas Biesecker, Steve Hill, and Dusan Odstrcil. Wang-Sheeley-Arge-Enlil Cone Model Transitions to Operations. *Space Weather*, 9(3):03004, March 2011. doi: 10.1029/2011SW000663.
- S. B. Pope. *Turbulent Flows*. Cambridge University Press, August 2000.
- Rayta A. Pradata, Sohom Roy, William H. Matthaeus, Jiaming Wang, Rohit Chhiber, Francesco Pecora, and Yan Yang. Observations of 1/f Noise at Mercury’s Solar Wind Using MESSENGER Data. *ApJL*, 984(1):L23, May 2025. doi: 10.3847/2041-8213/adc9b2.
- Elena Provornikova, Viacheslav G. Merkin, Angelos Vourlidas, Anna Malanushenko, Sarah E. Gibson, Eric Winter, and Charles N. Arge. MHD Modeling of a Geoeffective Interplanetary Coronal Mass Ejection with the Magnetic Topology Informed by In Situ Observations. *ApJ*, 977(1):106, December 2024. doi: 10.3847/1538-4357/ad83b1.
- Tuija Pulkkinen. Space Weather: Terrestrial Perspective. *Living Reviews in Solar Physics*, 4(1):1, December 2007. doi: 10.12942/lrsp-2007-1.

- I. G. Richardson and H. V. Cane. Near-Earth Interplanetary Coronal Mass Ejections During Solar Cycle 23 (1996 - 2009): Catalog and Summary of Properties. *Sol. Phys.*, 264(1):189–237, June 2010. doi: 10.1007/s11207-010-9568-6.
- Ian Richardson and Hilary Cane. Near-Earth Interplanetary Coronal Mass Ejections Since January 1996, 2024. URL <https://doi.org/10.7910/DVN/C2MHTH>.
- Yeimy J. Rivera, Samuel T. Badman, Michael L. Stevens, Jaye L. Verniero, Julia E. Stawarz, Chen Shi, Jim M. Raines, Kristoff W. Paulson, Christopher J. Owen, Tatiana Niembro, Philippe Louarn, Stefano A. Livi, Susan T. Lepri, Justin C. Kasper, Timothy S. Horbury, Jasper S. Halekas, Ryan M. Dewey, Rossana De Marco, and Stuart D. Bale. In situ observations of large-amplitude Alfvén waves heating and accelerating the solar wind. *Science*, 385(6712):962–966, August 2024. doi: 10.1126/science.adk6953.
- Sohom Roy, R. Chhiber, S. Dasso, M. E. Ruiz, and W. H. Matthaeus. von Karman Correlation Similarity of the Turbulent Interplanetary Magnetic Field. *ApJL*, 919(2):L27, October 2021. doi: 10.3847/2041-8213/ac21d2.
- Sohom Roy, R. Chhiber, S. Dasso, M. E. Ruiz, and W. H. Matthaeus. von Karman correlation similarity in solar wind magnetohydrodynamic turbulence. *Phys. Rev. E*, 105(4):045204, April 2022. doi: 10.1103/PhysRevE.105.045204.
- M. E. Ruiz, S. Dasso, W. H. Matthaeus, and J. M. Weygand. Characterization of the Turbulent Magnetic Integral Length in the Solar Wind: From 0.3 to 5 Astronomical Units. *Solar Physics*, 289:3917–3933, October 2014. doi: 10.1007/s11207-014-0531-9.
- E. Samara, C. N. Arge, R. F. Pinto, J. Magdaleníć, N. Wijsen, M. L. Stevens, L. Rodriguez, and S. Poedts. Calibrating the WSA Model in EUHFORIA Based on Parker Solar Probe Observations. *ApJ*, 971(1): 83, August 2024. doi: 10.3847/1538-4357/ad53c6.
- Chen Shi, Marco Velli, Roberto Lionello, Nikos Sioulas, Zesen Huang, Jasper S. Halekas, Anna Tenerani, Victor Réville, Jean-Baptiste Dakeyo, Milan Maksimović, and Stuart D. Bale. Proton and Electron Temperatures in the Solar Wind and Their Correlations with the Solar Wind Speed. *ApJ*, 944(1):82, February 2023. doi: 10.3847/1538-4357/acb341.
- D. Shiotani, G. P. Zank, L. Adhikari, P. Hunana, D. Telloni, and R. Bruno. Turbulent Transport in a Three-dimensional Solar Wind. *ApJ*, 837:75, March 2017. doi: 10.3847/1538-4357/aa60bc.
- Ruth Skoug, Dave J. McComas, and Heather A. Elliott. Effect of ace spacecraft repointing on swepam calculated moments. Technical report, ACE Science Center, California Institute of Technology, 2014. URL [https://izw1.caltech.edu/ACE/ASC/ACE\\_repointing.pdf](https://izw1.caltech.edu/ACE/ASC/ACE_repointing.pdf). Technical analysis memo; discusses CEM aging (post-2010) and Oct 23, 2012 repointing improving valid moments.
- Ruth M Skoug, JT Gosling, John T Steinberg, DJ McComas, CW Smith, NF Ness, Q Hu, and LF Burlaga. Extremely high speed solar wind: 29–30 october 2003. *Journal of Geophysical Research: Space Physics*, 109(A9), 2004.
- Charles W Smith, Jacques L’Heureux, Norman F Ness, Mario H Acuna, Leonard F Burlaga, and John Scheifele. The ace magnetic fields experiment. *Space Science Reviews*, 86(1):613–632, 1998.
- Igor V. Sokolov, Bart van der Holst, Rona Oran, Cooper Downs, Ilia I. Roussev, Meng Jin, Ward B. Manchester, IV, Rebekah M. Evans, and Tamas I. Gombosi. Magnetohydrodynamic Waves and Coronal

- Heating: Unifying Empirical and MHD Turbulence Models. *ApJ*, 764(1):23, February 2013. doi: 10.1088/0004-637X/764/1/23.
- Vishal Upendran, Mark C. M. Cheung, Shravan Hanasoge, and Ganapathy Krishnamurthi. Solar Wind Prediction Using Deep Learning. *Space Weather*, 18(9):e02478, September 2020. doi: 10.1029/2020SW002478.
- A. V. Usmanov, M. L. Goldstein, B. P. Besser, and J. M. Fritzer. A global MHD solar wind model with WKB Alfvén waves: Comparison with Ulysses data. *J. Geophys. Res.*, 105:12675–12696, June 2000. doi: 10.1029/1999JA000233.
- Arcadi V. Usmanov, Rohit Chhiber, William H. Matthaeus, Sohom Roy, and Melvyn L. Goldstein. A Unified Three-dimensional Magnetohydrodynamic Model of the Solar Corona, Solar Wind, and Global Heliosphere with Turbulence Transport. *ApJ*, 993(1):87, November 2025. doi: 10.3847/1538-4357/ae019c.
- Ilya G. Usoskin. A history of solar activity over millennia. *Living Reviews in Solar Physics*, 20(1):2, December 2023. doi: 10.1007/s41116-023-00036-z.
- B. van der Holst, I. V. Sokolov, X. Meng, M. Jin, W. B. Manchester, IV, G. Tóth, and T. I. Gombosi. Alfvén Wave Solar Model (AWSolM): Coronal Heating. *ApJ*, 782:81, February 2014. doi: 10.1088/0004-637X/782/2/81.
- Daniel Verscharen, Kristopher G. Klein, and Bennett A. Maruca. The multi-scale nature of the solar wind. *Living Reviews in Solar Physics*, 16(1):5, December 2019. doi: 10.1007/s41116-019-0021-0.
- Jiaming Wang, Rohit Chhiber, Sohom Roy, Manuel E. Cuesta, Francesco Pecora, Yan Yang, Xiangrong Fu, Hui Li, and William H. Matthaeus. Anisotropy of Density Fluctuations in the Solar Wind at 1 au. *ApJ*, 967(2):150, June 2024. doi: 10.3847/1538-4357/ad3e7a.
- Jiaming Wang, Francesco Pecora, Rohit Chhiber, Sohom Roy, and William H. Matthaeus. Interplanetary magnetic correlation and low-frequency spectrum over many solar rotations. *arXiv e-prints*, art. arXiv:2507.16053, July 2025.
- Y.-M. Wang and N. R. Sheeley, Jr. Solar Wind Speed and Coronal Flux-Tube Expansion. *ApJ*, 355:726, June 1990. doi: 10.1086/168805.
- Y.-M. Wang and N. R. Sheeley, Jr. Why Fast Solar Wind Originates from Slowly Expanding Coronal Flux Tubes. *ApJL*, 372:L45, May 1991. doi: 10.1086/186020.
- David F. Webb and Timothy A. Howard. Coronal Mass Ejections: Observations. *Living Reviews in Solar Physics*, 9(1):3, December 2012. doi: 10.12942/lrsp-2012-3.
- Kathryn Whitman, Ricky Egeland, Ian G. Richardson, Clayton Allison, Philip Quinn, Janet Barzilla, Irina Kitiashvili, Viacheslav Sadykov, Hazel M. Bain, Mark Dierckx, M. Leila Mays, Tilaye Tadesse, Kerry T. Lee, Edward Semones, Janet G. Luhmann, Marlon Núñez, Stephen M. White, Stephen W. Kahler, Alan G. Ling, Don F. Smart, Margaret A. Shea, Valeriy Tenishev, Soukaina F. Boubrahimi, Berkay Aydin, Petrus Martens, Rafal Angryk, Michael S. Marsh, Silvia Dalla, Norma Crosby, Nathan A. Schwadron, Kamen Kozarev, Matthew Gorby, Matthew A. Young, Monica Laurenza, Edward W. Cliver, Tommaso Alberti, Mirko Stumpo, Simone Benella, Athanasios Papaioannou, Anastasios Anastasiadis, Ingmar Sandberg, Manolis K. Georgoulis, Anli Ji, Dustin Kempton, Chetraj Pandey, Gang Li, Junxiang Hu, Gary P. Zank, Eleni Lavasa, Giorgos Giannopoulos, David Falconer, Yash Kadadi,

Ian Fernandes, Maher A. Dayeh, Andrés Muñoz-Jaramillo, Subhamoy Chatterjee, Kimberly D. Moreland, Igor V. Sokolov, Ilia I. Roussev, Aleksandre Taktakishvili, Frederic Effenberger, Tamas Gombosi, Zhenguang Huang, Lulu Zhao, Nicolas Wijsen, Angels Aran, Stefaan Poedts, Athanasios Kouloumvakos, Miikka Paassilta, Rami Vainio, Anatoly Belov, Eugenia A. Eroshenko, Maria A. Abunina, Artem A. Abunin, Christopher C. Balch, Olga Malandraki, Michalis Karavolos, Bernd Heber, Johannes Labrenz, Patrick Kühl, Alexander G. Kosovichev, Vincent Oria, Gelu M. Nita, Egor Illarionov, Patrick M. O’Keefe, Yucheng Jiang, Sheldon H. Ferreira, Aatiya Ali, Evangelos Paouris, Sigiava Aminafragia-Giamini, Piers Jiggins, Meng Jin, Christina O. Lee, Erika Palmerio, Alessandro Bruno, Spiridon Kasapis, Xiantong Wang, Yang Chen, Blai Sanahuja, David Lario, Carla Jacobs, Du Toit Strauss, Ruhann Steyn, Jabus van den Berg, Bill Swalwell, Charlotte Waterfall, Mohamed Nedal, Rositsa Miteva, Momchil Dechev, Pietro Zucca, Alec Engell, Brianna Maze, Harold Farmer, Thuha Kerber, Ben Barnett, Jeremy Loomis, Nathan Grey, Barbara J. Thompson, Jon A. Linker, Ronald M. Caplan, Cooper Downs, Tibor Török, Roberto Lionello, Viacheslav Titov, Ming Zhang, and Pouya Hosseinzadeh. Review of Solar Energetic Particle Prediction Models. *Advances in Space Research*, 72(12):5161–5242, December 2023. doi: 10.1016/j.asr.2022.08.006.

Daniel Wrench and Tulasi N. Parashar. Debiasing Structure Function Estimates from Sparse Time Series of the Solar Wind: A Data-driven Approach. *ApJ*, 987(1):28, July 2025. doi: 10.3847/1538-4357/ad6c6a.

Honghong Wu, Chuanyi Tu, Jiansen He, Xin Wang, and Liping Yang. Consistency of von Karman Decay Rate with the Energy Supply Rate and Heating Rate Observed by Parker Solar Probe. *ApJ*, 926(2): 116, February 2022. doi: 10.3847/1538-4357/ac4413.

G. P. Zank, L. Adhikari, P. Hunana, D. Shiota, R. Bruno, and D. Telloni. Theory and Transport of Nearly Incompressible Magnetohydrodynamic Turbulence. *ApJ*, 835:147, February 2017. doi: 10.3847/1538-4357/835/2/147.

Y. Zhou, W. H. Matthaeus, and P. Dmitruk. Colloquium: Magnetohydrodynamic turbulence and time scales in astrophysical and space plasmas. *Reviews of Modern Physics*, 76:1015–1035, December 2004. doi: 10.1103/RevModPhys.76.1015.